Gilman Springs Road Phase 6 Safety Project

From 8,920 Feet S/O Alessandro Boulevard To 5,340 Feet S/O Bridge Street

Eastern Moreno Valley and Gilman Hot Springs Areas

Project No. C2-0161

Federal Aid No. HSIPL-5956 (263)

Bridge Street Crossing
Hydraulics and Scour Analysis Report
Dated February 2024

Notice regarding this Report:

This report is provided for reference only.

Although this information represents the latest information available, the County of Riverside Transportation Department does not guarantee the accuracy of this data.

Gilman Springs Road

Bridge Street Crossing Hydraulics and Scour Analysis

Prepared for:

County of Riverside Transportation Department
4080 Lemon Street
Riverside, CA 92502-1629

Prepared by:

Tetra Tech
17885 Von Karman Ave, Suite 500
Irvine, California 92614

FEBRUARY 2024

THIS PAGE INTENTIONALLY LEFT BLANK

Table of Contents

Figures

Tables

THIS PAGE INTENTIONALLY LEFT BLANK

1.0 Introduction

Riverside County Transportation Department is looking to widen Gilman Springs Road from State Route 60, to State Route 79. As part of the improvements, the culvert crossing at Bridge Street is being replaced to allow for animal crossings under the roadway. Tetra Tech was contracted by NCM Engineering, under contract with Riverside Transportation Department, to evaluate the hydraulic conditions at the bridge crossing and to evaluate potential scour to inform bridge replacement design for a wildlife undercrossing. This report catalogs the existing condition and proposed condition analysis results.

The unnamed canyon crossing immediately north of Bridge Street at Gilman Springs Road flows in a predominantly north to south direction through unincorporated Riverside County, south of the city of Moreno Valley, and north of the cities of San Jacinto and Hemet. Its headwaters are located approximately 1.3 miles to the northeast in the series of hills known as the Badlands between the San Jacinto Valley and Beaumont. **Figure 1-1** shows the location of the Bridge Street crossing and its associated canyon and watershed included in this study. Within this report we will refer to the canyon as Bridge Street Canyon.

Bridge Street Canyon is a sand bed channel along its downstream length in the project area. Upstream of the crossing it is a natural watercourse with a defined canyon channel. Downstream of the crossing the slope of the channel is decreasing as it approaches the flats surrounding Mystic Lake. Here the creek has been excavated to direct flow away from Bridge Street. This roughly excavated channel downstream of the crossing slowly reduces in size until it disappears about 900-feet downstream where it becomes open terrain. The crossing generally represents the apex of the canyon's alluvial fan, which can be seen in the topography around Bridge Street.

Within this report, reference will be made to the right and left bank. These directions are based on an orientation looking downstream along the channel. The right bank is the northwest bank and left bank is the southeast bank.

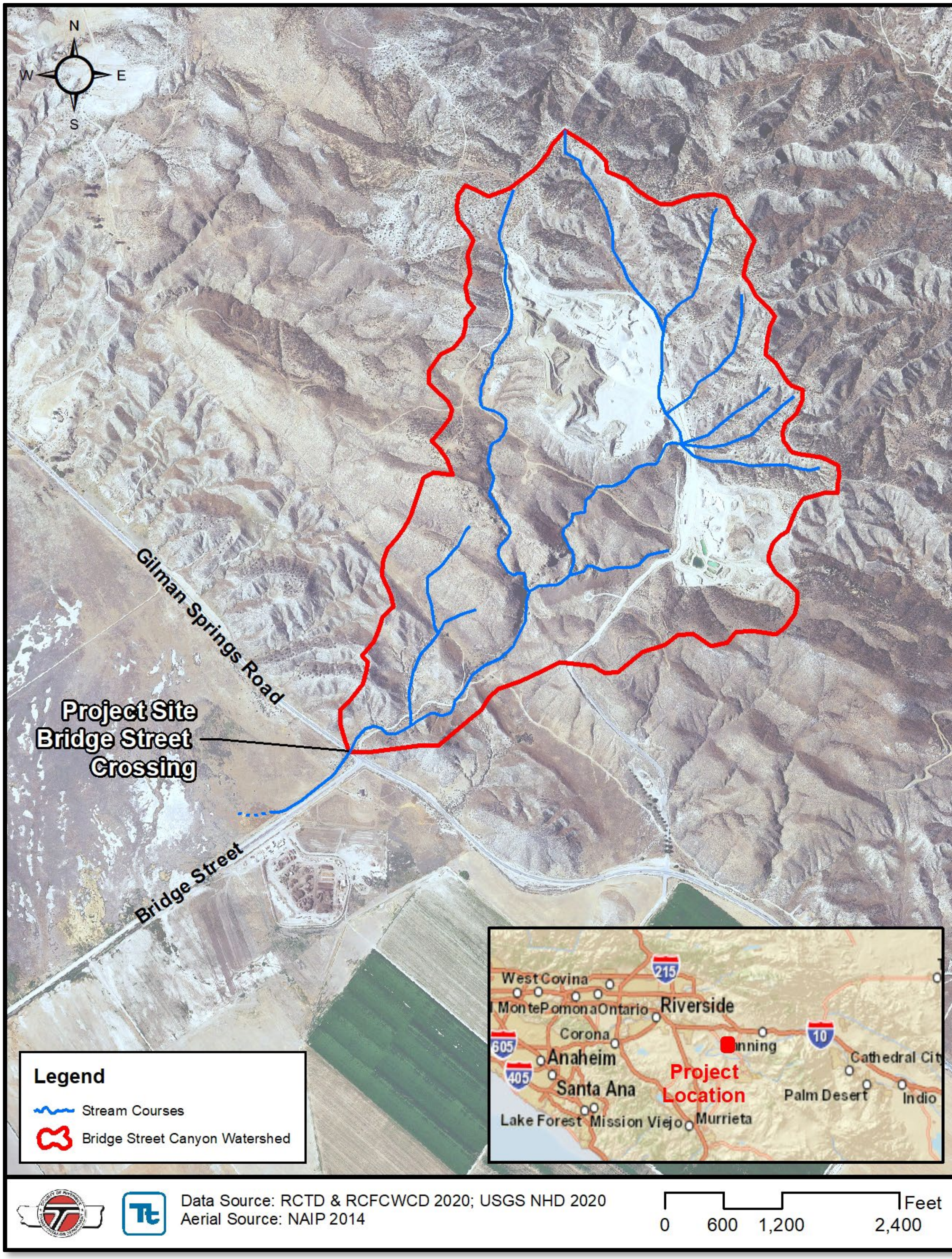

Figure 1-1 – Bridge Street Crossing Location Map

2.0 Data Collection

This section lists the drawings and reports used to support the hydrologic and hydraulic engineering analyses for the study. Except for the GIS topography, these are found in Appendix A.

2.1 As-built/Construction Drawings/Topography

- *Bridge Street Road Widening,* Drawing No. 926-UU, Sheet 25 of 43, prepared by Riverside County Transportation Department. As-built drawings dated February 2002.
- *Topographic LiDAR Terrain*. Provided by Riverside County Flood Control & Water Conservation District. Data acquired in 2014.
- *Wildlife Crossing - Bridge Cross Section Profile Contours,* prepared by NCM Engineering. Proposed drawings August 31st, 2020.

3.0 Hydrology

The hydrologic analysis was performed according to the procedures outlined in the Riverside County Flood Control & Water Conservation District Hydrology Manual (RCFC&WCD 1978). The RCFC&WCD approved Advanced Engineering Software (AES) Synthetic Unit Hydrograph computer program was used in the development of the 100-year hydrology for the Bridge Street Canyon crossing.

3.1 Topographic Data & Drainage Area

USGS topographic maps were used for initial delineation of the watershed. The boundaries were cross checked and verified with LiDAR derived terrain data later provided by RCFC&WCD. The drainage area is estimated to be 425 acres (**Figure 1-1**).

3.2 Methodology

The Synthetic Unit Hydrograph method is used in performing hydrologic analysis for drainage areas in excess of 300 acres, but less than 500 acres, per RCFC&WCD Hydrology Manual (RCFC&WCD 1978), and was utilized in this study.

3.3 S-graph

An S-graph represents the basic time-runoff relationship for a watershed type in a form suitable for application to ungauged basins. Four S-graphs are used to represent the runoff characteristics of watersheds in western Riverside County. These S-graphs are titled Valley, Foothill, Mountain, and Desert, respectively. The Foothill curve is suitable for small watersheds with extreme slopes, or for confined valley areas surrounded by steep foothills, therefore, it is used in this hydrologic analysis.

3.4 Watershed Lag Time

Watershed lag time is used to relate an S-graph to a particular basin for the purpose of deriving a Synthetic Unit graph for that basin. Lag for a drainage area is defined as the elapsed time in hours from the beginning of unit effective rainfall to the instant that the summation hydrograph for the concentration point of an area reaches 50 percent of ultimate discharge. Lag can be calculated from the physical characteristics of a drainage area by the empirical formula:

$$Lag\ (hours) = 24 \cdot \bar{n} \cdot (\frac{L \cdot Lca}{S^{1/2}})^{0.38}$$

Where:

$\bar{n}$ = The visually estimated mean of the n (Manning's formula) values of all collection streams and channels within the watershed;

L = Length of longest watercourse, miles;

Lca = Length along longest watercourse, measured upstream to a point opposite the centroid of the area, miles; and

S = Overall slope of longest watercourse between headwaters and the collection point, feet per mile.

Watershed lag time is estimated to be 0.262 hours as shown in **Table 3-1**.

Table 3-1 – Watershed Lag Time (hours)

L (ft)/(mi)	Lca (ft)/(mi)	Elevation Drop[1] (ft)	S (ft/mile)	$\bar{n}$[2]	Lag (hours)
9088/1.72	4462/0.85	740	430	0.030	0.262

1. Elevation difference between headwaters and the collection point.
2. Per Plate E-3 of RCFC&WCD Hydrology Manual (RCFC&WCD 1978).

3.5 Land Use/ Land Cover

Based on the Riverside County general plan land use GIS coverage (RC 2020), the drainage area consists of open space with the rural and mineral resources sub-categories. Since the drainage area is designated as open spaces, the National Land Cover Dataset (NRCS 2011) was used to estimate the vegetation cover. Land cover of the drainage area consists of barren land, developed/open space, herbaceous, and shrub/scrub per National Land Cover Dataset (NRCS 2011). The "poor" quality cover type is assumed in this analysis because the drainage area has less than 50 percent of ground surface with plant cover or brush and tree canopy. Watershed land use and land cover types are shown on **Figure 3-1** and **Figure 3-2**.

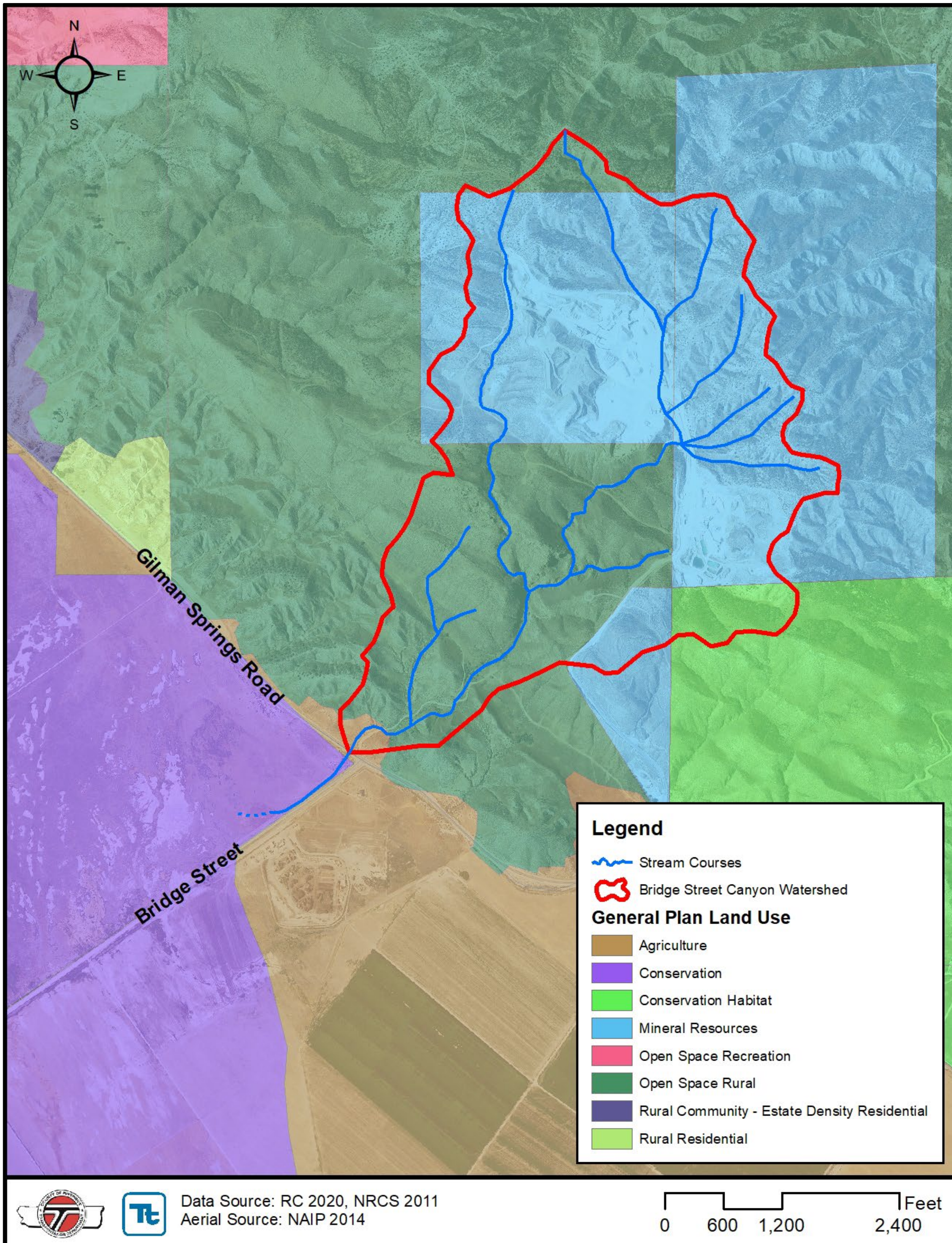

Figure 3-1 – Land Use Map

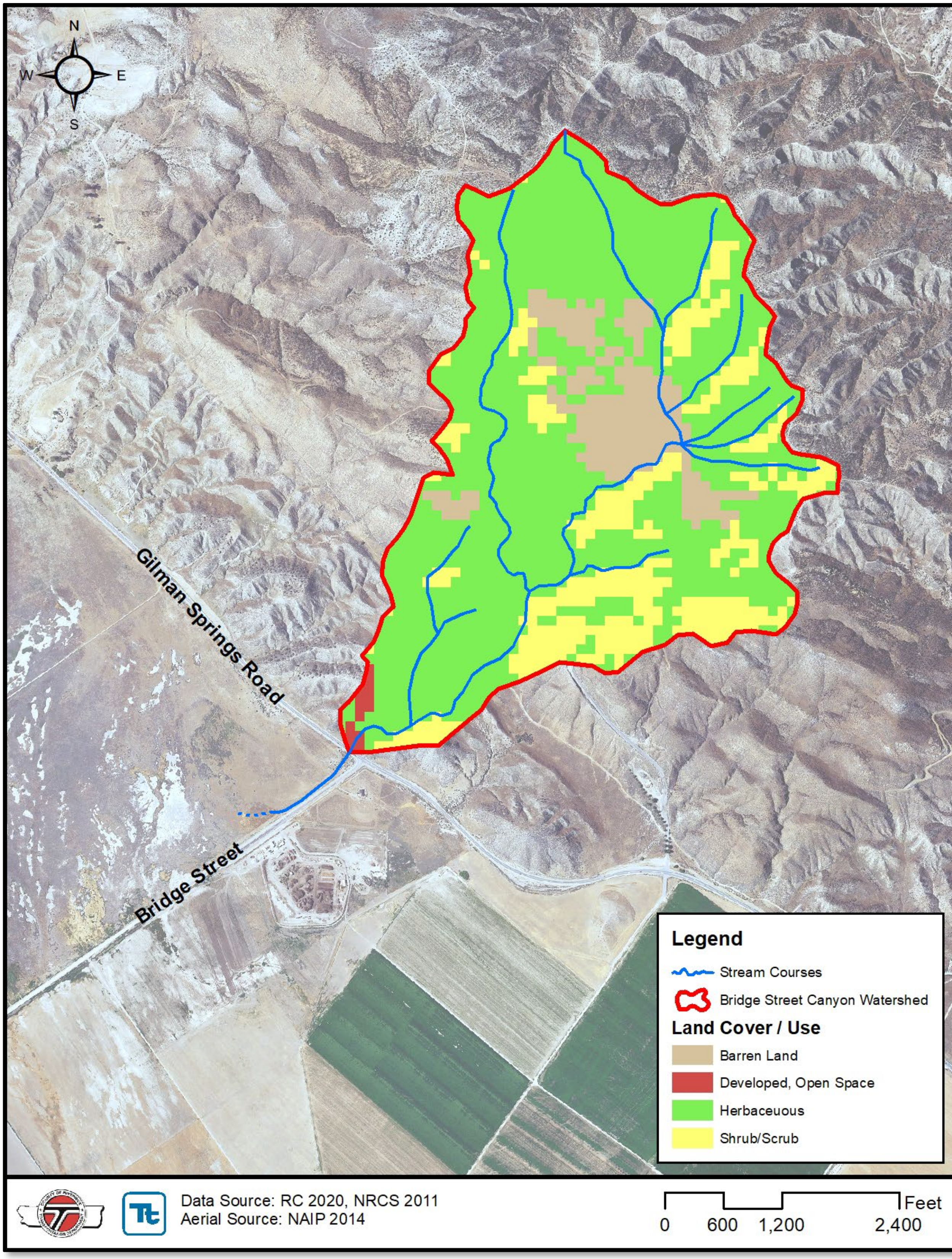

Figure 3-2 – Land Cover Map

3.6 Infiltration

Infiltration is the process of water entering the soil surface. In the RCFC&WCD design hydrology manual, infiltration is expressed as the rate in inches per hour at which precipitation enters the soil surface and is stored in the subsurface structure. RCFC&WCD Hydrology Manual has classified the soils into four hydrologic soils groups as: Group A – low runoff potential; Group B – moderate infiltration rates; Group C – slow infiltration rates; and Group D – high runoff potential. The drainage area in this analysis is dominated by hydrologic soil group D with small areas of hydrologic soil groups A and B. Watershed hydrologic soil groups are shown on **Figure 3-3**.

Antecedent moisture condition (AMC) has a major effect on the runoff potential of a particular soil-cover complex. For this analysis, AMC II is used for the 100-year frequency storm according to RCFC&WCD Hydrology Manual (RCFC&WCD 1978).

National Land Cover Dataset land cover types are mapped into RCFC&WCD Hydrology Manual cover types and runoff index numbers and presented in **Table 3-2**.

Table 3-2 – Land Cover Types

National Land Cover Dataset Land Cover	RCFC&WCD Hydrology Manual Cover Type	Runoff Index Numbers (AMC II)			
		A	B	C	D
Barren Land	Barren	78	86	91	93
Developed, Open Space; Herbaceous	Grass, Annual or Perennial[1]	67	78	86	89
Shrub/Scrub "Poor" quality cover type.	Open Brush[1]	62	76	84	88

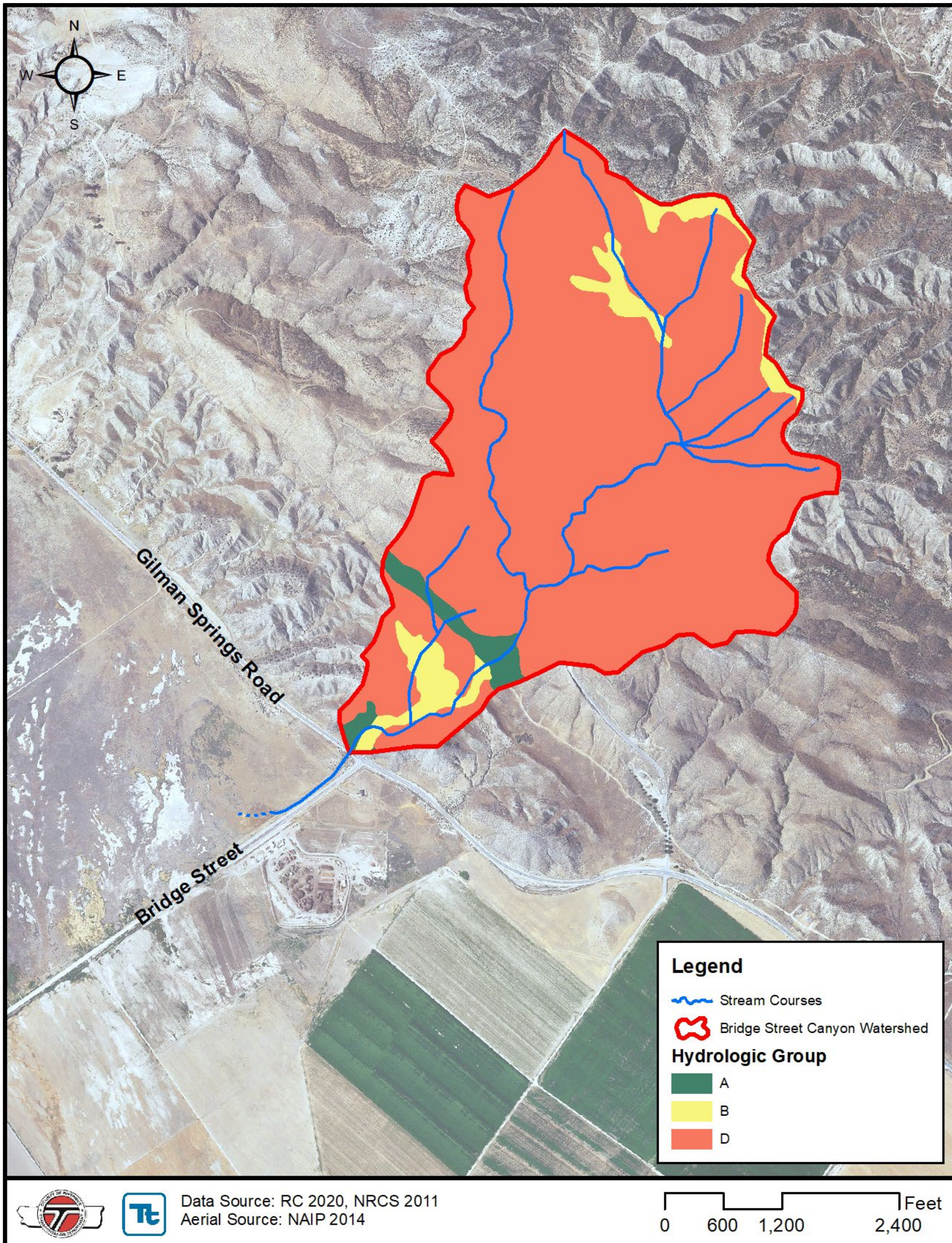

Figure 3-3 – Soil Classification Map

3.7 Precipitation

Precipitation point rainfall data at the watershed centroid are obtained from the Precipitation-Frequency Atlas of the United States, Volume 6 Version 2.3 : California (NOAA 2014) and listed in **Table 3-3**. In this hydrologic analysis, the 50-, 100-, and 500- year 1-hour, 3-hour, and 6-hour duration storm events are used in developing the peak discharges.

Table 3-3 – Point precipitation frequency estimates (inches)

Duration	Average Recurrence Interval (years)							
	2	5	10	25	50	100	200	500
5-min	0.131	0.178	0.219	0.283	0.337	0.399	0.469	0.578
30-min	0.347	0.470	0.581	0.748	0.893	1.06	1.24	1.53
60-min	0.513	0.695	0.858	1.11	**1.32**	***1.56***	1.84	**2.26**
2-hr	0.726	0.949	1.14	1.43	1.67	1.94	2.23	2.67
3-hr	0.884	1.14	1.36	1.68	**1.95**	***2.24***	2.55	**3.02**
6-hr	1.25	1.59	1.88	2.30	2.64	2.99	3.38	3.92
12-hr	1.67	2.15	2.55	3.11	3.55	4.01	4.50	5.18
24-hr	2.24	2.94	3.52	4.32	**4.95**	***5.60***	6.28	**7.23**

3.8 50-, 100-, and 500- year Hydrology

Computed 50-, 100-, and 500- year peak discharges are listed in **Table 3-4**. Developments of the hydrologic parameters and AES computer model output files are provided in Appendix B.

Table 3-4 – 50-, 100-, and 500- year Peak Discharges

Storm Duration (hr)	Time to Peak (hr)	Peak Flow (cfs)	Runoff Volume (af)
50-year Storm Event			
1	1.08	835	40.21
3	2.75	536	52.26
6	5.67	473	60.47
24	13.75	211	88.48
100-year Storm Event			
1	1.08	998	48.5
3	2.75	626	62.5
6	5.67	545	72.7
24	13.41	247	106.2

Storm Duration (hr)	Time to Peak (hr)	Peak Flow (cfs)	Runoff Volume (af)
500-year Storm Event			
1	1.08	1511	75.98
3	2.75	905	99.42
6	5.67	774	123.98
24	13.41	368	200.73
Notes: cubic feet per second (cfs); acre-feet (af)			

4.0 Hydraulic Model

HEC-RAS models were developed to evaluate the existing condition and proposed concept design plan for the replacement of the bridge culvert with a wider bridge deck. Version 5.0.7 of HEC-RAS was used. The following inputs were developed for the hydraulic model.

4.1 Cross Sections

Utilizing available as-built condition plans (for the existing culvert/bridge), cross sections were placed immediately upstream and downstream of the existing crossing, with additional cross sections upstream 2000 feet, and downstream 300 feet, spaced 50 feet apart. More cross sections were included in shorter increments close to the bridge itself and at the upstream end of the model. The cross sections were cut from the existing topography provided by RCFC&WCD. The data was collected with LiDAR in 2014. The initial cross sections were used in an existing condition model. In the proposed condition model, the culvert was replaced by the proposed bridge, and warped wingwall and grading geometry to reflect the proposed design at the approach and outlet.

4.2 Culvert/Bridge

The modeling parameters for the existing condition culvert along Gilman Springs Road was built from the as-built plans of the culvert as well as verification in field observations. This was coded as a culvert into the model with an approach skew of 15 degrees, n-value of 0.012 for concrete, with 90 degree chamfered edge headwall.

The modeling parameters for the proposed condition culvert was built from the proposed plans of the new culvert and bridge deck. These were coded as cross sections with lids. The upstream and downstream ends of the warped wingwall were coded in and extra cross sections were interpolated between them and the bridge to generate the warped shape. Existing cross sections in the graded area just outside the warped wingwalls were updated.

4.3 Starting Water Surface Elevation

The upstream boundary condition was set to critical depth in the HEC-RAS model. The downstream boundary condition was set to normal depth with a local slope of 0.02 generalized from the topographic LiDAR data in the downstream excavated channel.

The flow regime was set to supercritical due to the steepness of the channel slope and high Froude numbers displayed in the initial model runs.

4.4 Manning's n-value

A Manning's n-value (roughness coefficient) represents the resistance to the flood flows in channels and floodplains. In sandy and vegetated natural channels and floodplains, the greatest proportion of roughness is caused by trees, vines, and brush, plus the natural bed material. Cowan (1956) developed a procedure for estimating the effects of these factors to determine the composite n-values as follows:

$$n = (n_b + n_1 + n_2 + n_3 + n_4) \bullet m$$

Where

n_b = a base value of n-value for a straight, uniform, smooth channel in natural materials,

n_1 = a correction factor for the effect of surface irregularities,

n_2 = a value for variation in shape and size of the channel cross section,

n_3 = a value for obstructions,

n_4 = a value for vegetation and flow conditions, and

m = a correction factor for meandering of the channel.

In order to define the composite n-values associated within the bed and banks, the adjustment values for factors that affect roughness of floodplains presented by Arcement and Schneider (1989) was used in conjunction with the Cowan (1956) composite n-value estimation procedures. Due to the channel and banks being mostly inundated in peak flows based on the channel geometry, a single n-value was used for each entire cross-section.

Based on the field observations, the channel and bank composite Manning n-values were estimated in **Table 4-1**. The base value, n_b, of 0.03 was selected for sand bed channel based on the coarse sand composition; the degree of irregularity, n_1, was assumed to be smooth as the channel alternates between scalloped or non-irregular; the variation of the shape and size, n_2, the natural channel shows general uniformity in geometry; the effect of osbstructions, n_3, is near negligible with occasional stumps, roots, stones, etc.; the amount of the vegetation within the channel/overbank, n_4, of 0.026 was selected for vegetation of somewhat large amount as vegetation in the form of grasses and shrubs would range from completely to partially submerged depending on whether it was on the banks or closer to the channel thalweg; no degree of meandering, m, was assumed given the canyon conditions and excavated channel downstream.

Table 4-1 - Summary of n-value determination

	Manning's n-value		
	Type	**Selected**	**Range**
Base Channel, n_b	sand	0.03	0.026-0.035
Degree of Irregularity, n_1	smooth	0.00	
Variation of Cross Section , n_2	gradual	0.00	
Effects of Obstructions, n_3	negligible	0.004	0.000 - 0.004
Amount of Vegetation, n_4	large	0.026	0.025 - 0.05
Degree of Meandering, m	none	1	
Composite n-value = $(n_b + n_1 + n_2 + n_3 + n_4) * m$		0.06	

Per **Table 4-1**, the composite n-value expected in Bridge Street Canyon was estimated to be 0.06 for the channel and banks. This factor is driven by the amount of vegetation and sand bed. For reference, **Figure 4-1** and **Figure 4-2** show typical vegetation distributions downstream and upstream of the culvert, and they demonstrate how at peak flow condition there would be no real differentiation between a channel and floodplain for separate n-values.

Figure 4-1 – Grasses and Brush in channel and overbank Downstream

Figure 4-2 - Grasses and Brush in channel and overbank Upstream

In the culvert for the existing condition model, n-value was set to 0.012 for concrete. This value was also applied to the warped wingwall side slopes for the proposed condition model and the sidewalls of the replacement bridge.

In the proposed condition model, the design required different n-values for different sections of the system. Initial n-values for the grouted stone and stone channel bed at the upstream and downstream ends of the wingwalls is 0.045, with the banks remaining at 0.06. At the concrete wingwalls, the value is set at 0.012. For the sand channel bed through the structure a base n-value of 0.03 should not be utilized given the sand/soil cover will mobilize and scour out during storm peak flows. Although this would expose the flow to the concrete base with a lower n-value (0.012), which would thus accelerate the flow, such a low n-value does not account for the roughness inherent in flows laden with sediment passing through the system. Based on analyses in Section 6.5, the sediment laden concrete undercrossing bed n-value will be 0.023.

5.0 Hydraulic Analysis

The existing and proposed condition model were prepared and run. Results of the analysis are shown in tables in Appendix C and are summarized below.

5.1 Existing Condition

The existing condition box culvert is a 12'W x 6'H reinforced concrete box (RCB) with a length of 72.4 feet. It has chamfered inlet edges and flow approaches the culvert with approximately 15-degree skew.

There is a significant channel grade break about 1000-ft upstream. Within this approach reach channel flow area in the 100-yr 1-HR event generally is around 110-sqft with velocities of 10-12 feet per second (fps). Hydraulic depths in the reach averages 2.3-ft with average maximum depths of 3.9 feet. Velocities through the culvert are approximately 14 fps at the inlet, and 17.5 fps at the outlet, driven by the low n-value of the concrete culvert and the small cross section area. Downstream of the culvert, the 100-yr 1-HR event results are generally similar to upstream, though the maximum average depth is 1.5 feet greater and there is more variability in the velocities, flow area, and depths due to the roughly excavated channel being uneven.

The system is highly sensitive to differences/changes in n-value, and if the system had its vegetation scoured out, a sensitivity run with n-values of 0.03 for a sand channel only, shows that velocities in the natural channel mimic those found in the culvert itself, with the highest velocities entering the culvert (approximately 17 fps), with similar velocities immediately downstream of the culvert (approximately 18 fps). **Figure 5-1** on the following page shows the water surface elevations and profiles of the existing bridge/culvert crossing.

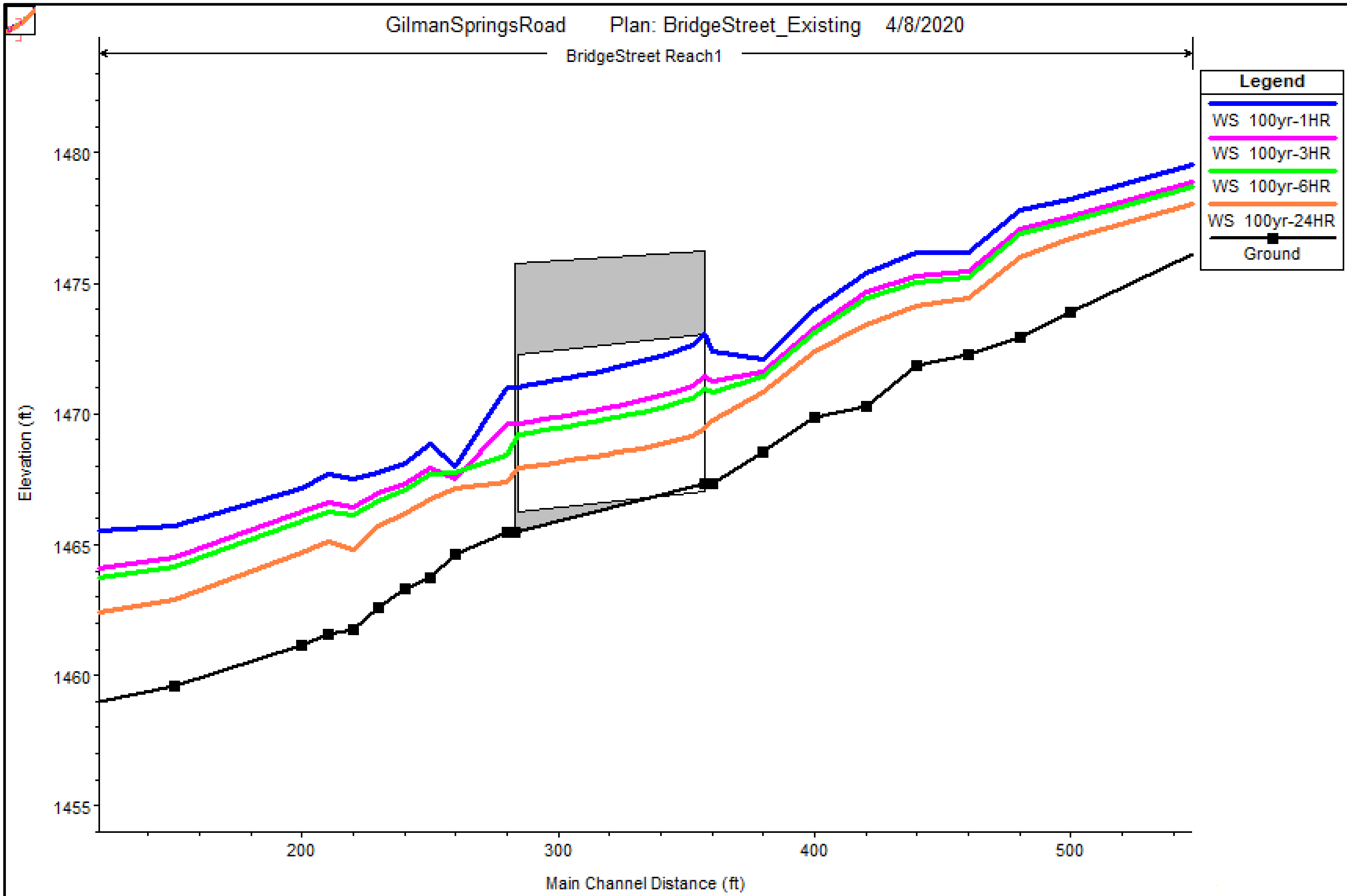

Figure 5-1 – Existing Condition Culvert Profile and WSELs

5.2 Proposed Condition

The proposed condition rectangular bridge with buried slab is a 26'W x 7.5'H, effectively a reinforced concrete box (RCB) with a length of 72.4 feet. It has a warped wingwall approach and outlet. The proposed buried slab and approach/exit bed/bank protection rip rap will be buried under 1.5 to 3-feet of soil. The bed of the material and final grading with concrete side walls was modeled as proposed. Manning's n-values for the upgraded reach of the system were set to the following:

Table 5-1 - Summary of Proposed Design Manning's n-values

Manning's n-value		
	Note	**Value**
Graded Channel	Sandy	0.023*
Wingwalls (rough concrete)	Concrete	0.012
Other Natural Channel	Existing Bed	0.06
Stone Protection	Rock	0.045

*Calculated mobile bed n-value (between just concrete and just sand n-values)

Note that if vegetation gets established in the sand bed, expected to deposit during low flows, the main channel n-value may increase upstream and downstream of the bridges. Severe storms with scour however should remove much of this vegetation.

The upstream and downstream ends of the buried rip rap (from natural bed to the warped wingwall concrete inlet) creates significant channel grade breaks at the end of the warped wingwall and at the beginning of the rip rap. Flow will drop from the natural channel, across the grading and bed protection to the inlet approach (~20 feet). Then the flow dynamics change in the warped wingwall approach to the bridge (~20 feet). **Table 5-2** below summarizes the results within these two sub-reaches, as well as the bridge and the outlet sub-reaches and the natural channel immediately downstream. **Figure 5-2** on the following page shows the water surface elevations and profiles of the design bridge crossing.

Table 5-2 - Summary of Proposed Condition 1Hr-100yr Hydraulics

Sub-Reach	Stationing	Ave Velocity (fps)	Ave Flow Area (sq ft)	Ave Hydraulic Depth (ft)	Ave Max Depth (ft)
Graded Approach w/RipRap	19+59.1 to 19+25.3	16.5	69.9	2.5	2.6
Warped Wingwall Inlet	19+23.7 to 19+07.9	17.5	57.3	2.1	2.3
Bridge	19+02.7 to 18+30.2	13.4	75.5	3.3	3.3
Warped Wingwall Outlet	18+24.9 to 18+14.2	13.2	75.9	2.6	3.0
Downstream w/RipRap	18+05.4 to 17+76.5	12.8	93.0	3.4	3.4

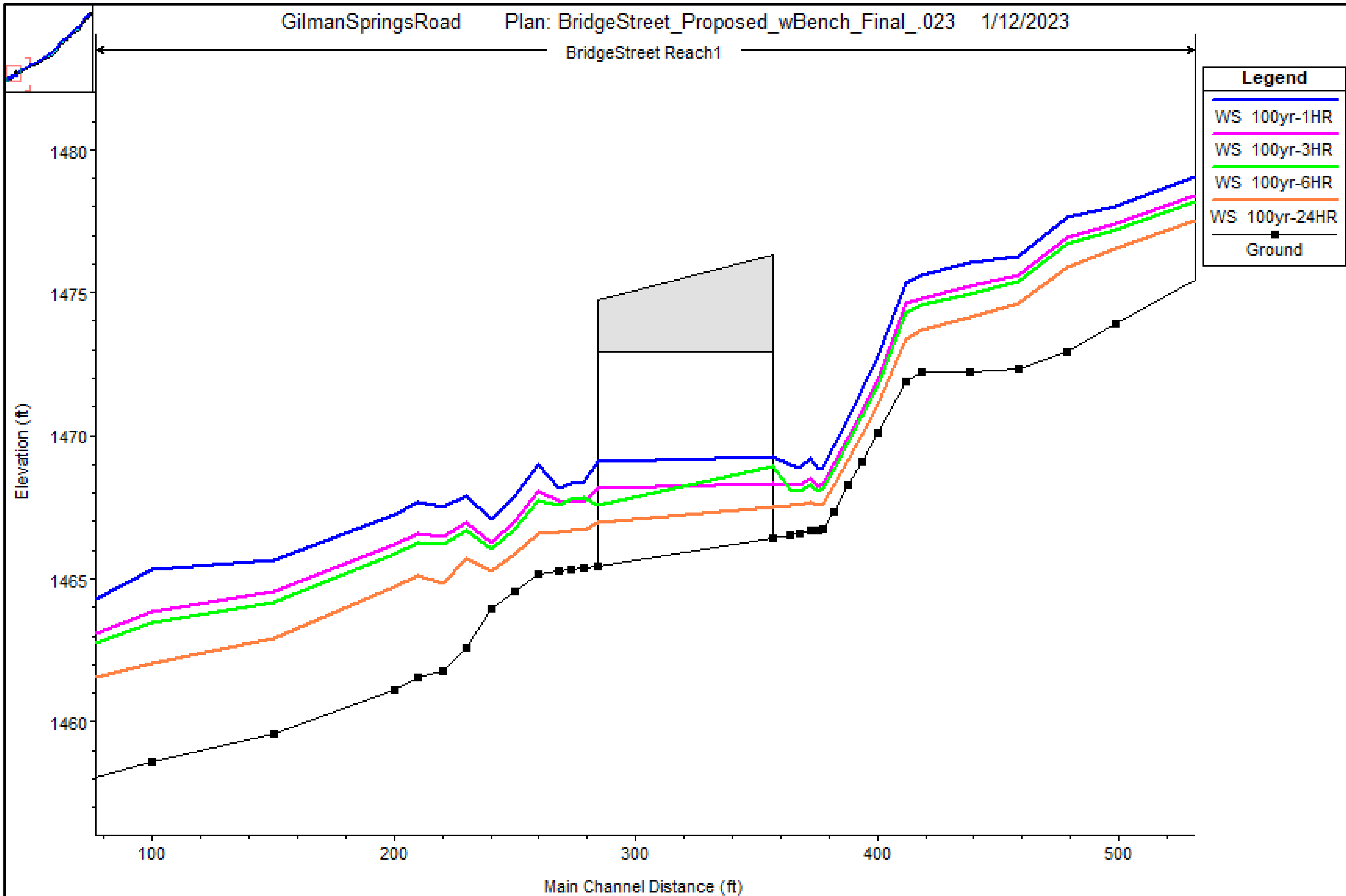

Figure 5-2 – Proposed Condition Culvert Profile and WSELs

These results, being based on the final design, show some differences with the original preliminary design grading. The preliminary design, where the concrete wingwall entrance was steeper into and out of the bridge lead to lower slopes in the proposed rock protected area upstream and downstream of the wingwall approaches and lower velocities in the areas of proposed grading with rock.

The changes included in the final design increase velocities in the rock protected areas by modifying the slopes in these reaches. The scour analysis and recommendations have been updated in Section 8.0.

5.3 Proposed Condition – 2D Cross Check

As a cross check to the 1D HEC-RAS analysis above, to verify hydraulic dynamics, particularly the local velocities and water surface elevations, a 2D model was created in HEC-RAS utilizing the final design surface and assigning the same n-values for the design features. A comparison of the results along the 1D model flow line is shown in the following two charts, focused on the 100-YR 1-HR events only as it provides the highest peak discharge. As can be seen, the velocities in the 2D model are generally higher where slopes are more consistent, but the peak velocities at the rock transitions spike more in the 1D model.

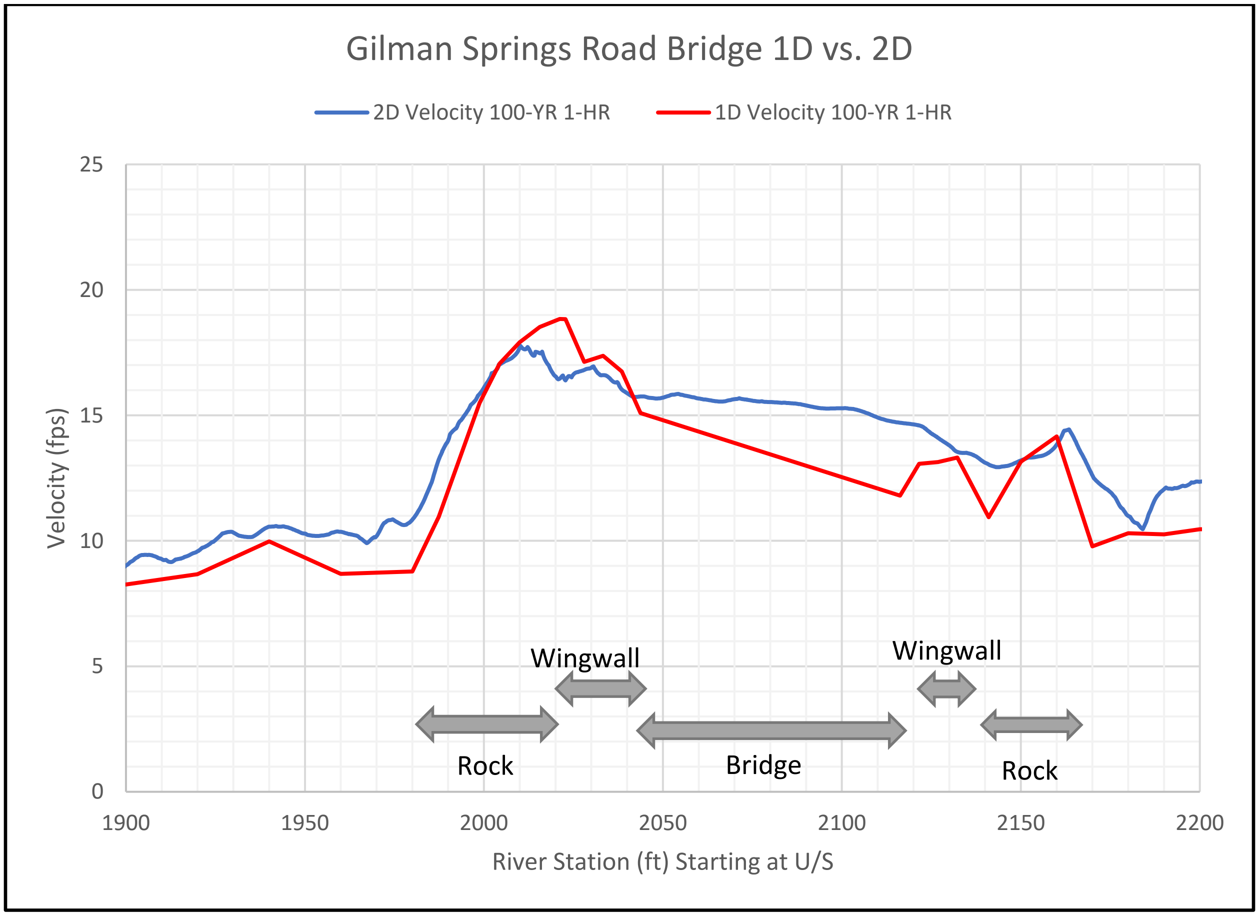

Figure 5-3 – 1D vs. 2D Velocities in 100-YR 1-HR Event

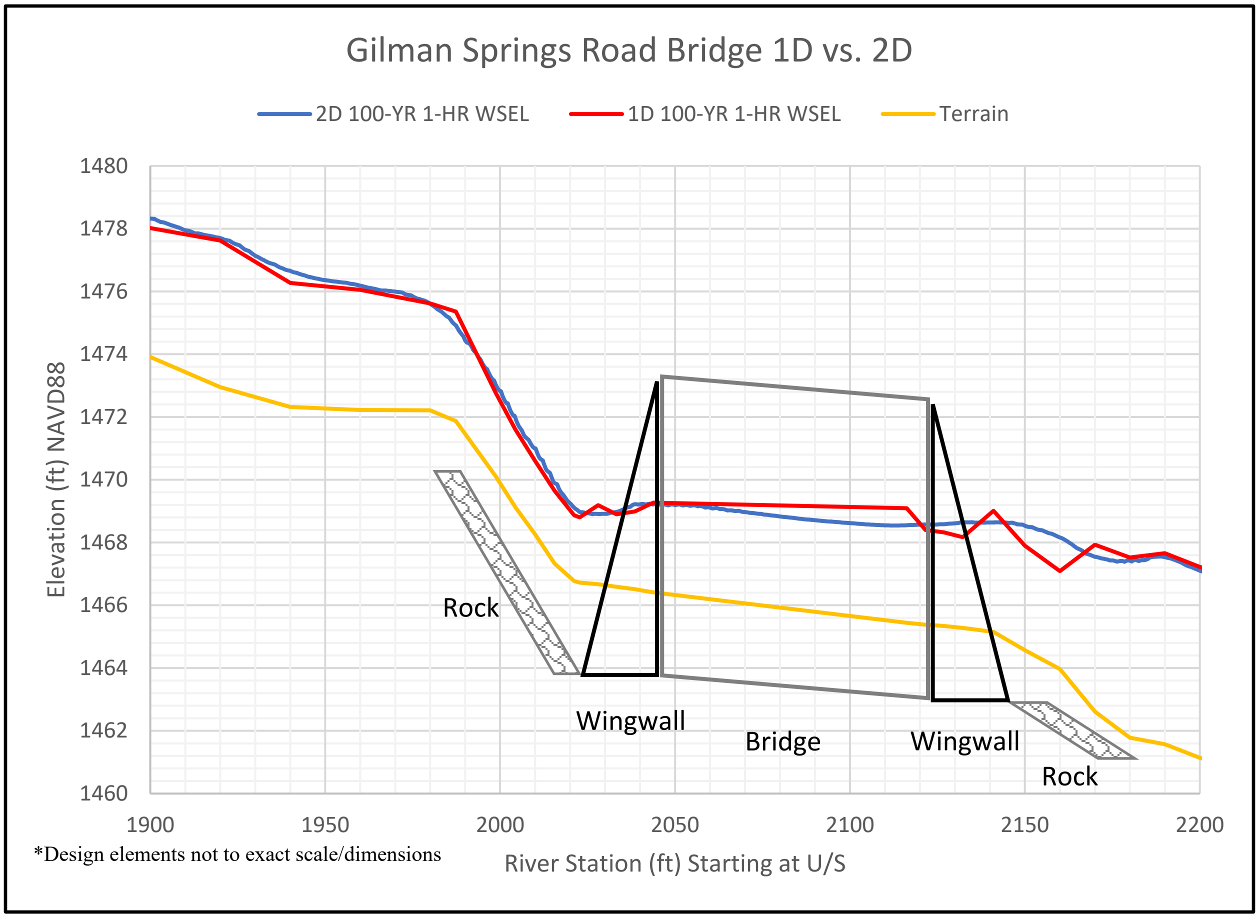

Figure 5-4 – 1D vs. 2D WSEL in 100-YR 1-HR Event

The 1D and 2D water surface elevation results are consistent, with minor differences where there are significant channel shape change transitions. The flow through the bridge is captured more accurately by the 2D model, as well as the transitions between changing cross section geometries and n-values. This is also notable in the velocities where the 2D model overcomes the limitations of 1D models with variable n-values and geometry transitions.

6.0 Sediment-transport Analysis

A sediment-continuity analysis was conducted to evaluate the sediment loads along the project reach of the channel under proposed conditions, and to assess the potential for long-term channel degradation downstream from the bridge crossing. The analysis provides an understanding of the overall sediment balance between the upstream sediment supply and the reach downstream from the crossing. To conduct the sediment-continuity analysis, reach-averaged hydraulic data from the model and bed-material information were used as input to an appropriate sediment-transport formula to develop discharge versus sediment-transport capacity rating curves. The rating curves were then integrated over the 1-hour, 6- hour and 24-hour 100-year storm hydrographs to estimate the sediment volumes transported along the reaches up- and downstream from the crossing associated with each hydrograph. The sediment-continuity analysis was performed for each storm event by comparing the bed-material transport capacity of the reach below the crossing to the bed-material supply from the upstream reach. The results of the sediment-transport analyses were compared to the computed bridge scour depths to inform the scour countermeasure design.

6.1 Sediment Gradation

Three sediment samples were taken to inform the bed gradation of the system. One 200-ft downstream of the culvert, to capture changes in fines passing through and settling (Boring GB-03). Two were taken upstream, one 300-ft upstream, and a second approximately 1000-ft upstream, above a tributary entering the system, to see if the gradation changed significantly (Borings GB-02 and GB-01 respectively). There was no significant change upstream of the tributary, so the samples reflected the mainstem of the watershed approaching the bridge. The upstream samples were classified as brown poorly graded sand with gravel, while the downstream sample was mostly the same but absent the gravel. Soil gradation lab sieve results are found in Appendix D.

6.2 Sediment-transport Formula Selection

The gradations from the three bed material samples discussed above were used as input to the computation of the sediment rating curves. Each of these samples included a small percentage (3% to 5%) of silt and clay. This fine material will be transported as wash load and does not represent the bed material load. As such, the gradations were adjusted to censor the silt/clay fractions. The adjusted gradations are shown in **Figure 6-1**. Sample GB-01, located downstream from the bridge, has a median diameter (D50) of 0.38 mm and includes 3 percent gravel. The samples upstream from the crossing (GB-02 and GB-03) are somewhat coarser, with a D50 of between 0.61 and 0.67 mm and about 20-percent gravel.

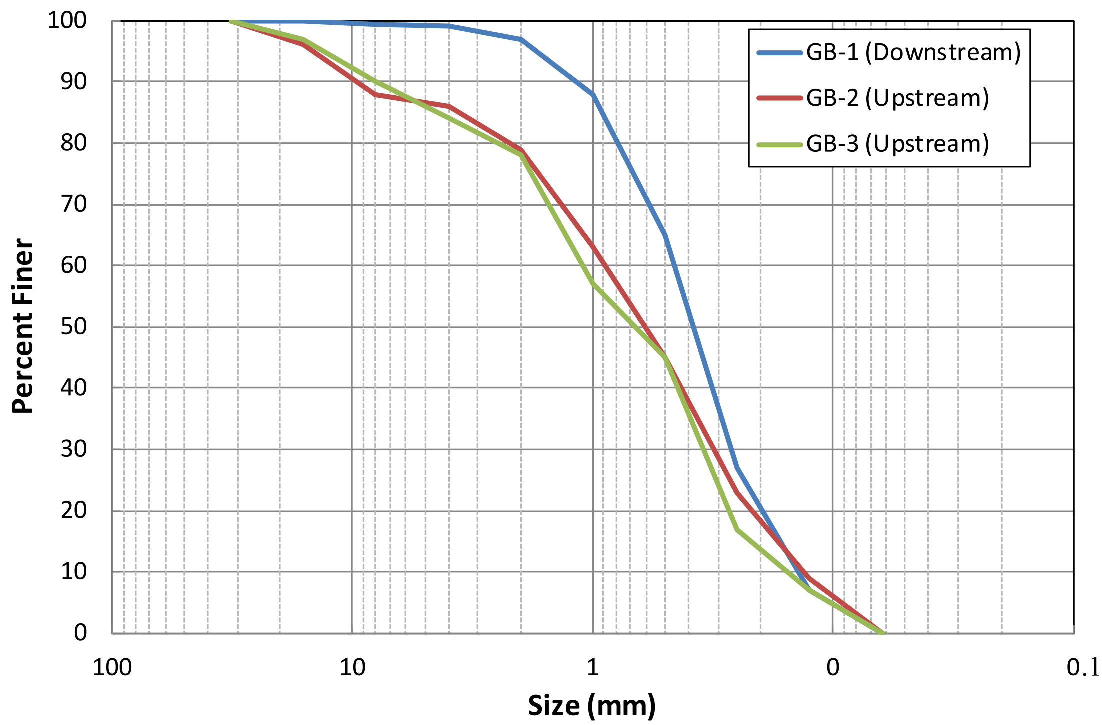

Figure 6-1 - Adjusted sediment gradations with censored fine (silt/clay) material content for the three bed material samples collected along the project reach.

Selection of the formula used to compute the bed-material transport capacity rating curves for the supply and downstream reaches was based on the range of bed-material sizes, hydraulic characteristics within the overall study reach, and previous experience with similar channels. A range of functions could be applicable to this study reach due to the varying hydraulic and bed-material characteristics along both reaches. Sediment transport capacity is the measure of how much of a particular grain class a hydrodynamic condition can transport. The transport capacity is computed by selecting one of a large number of transport functions. For this project, a range of functions were initially considered, including:

- Engelund and Hansen (1967), a total load function developed from flume studies using sand-size sediment. Median sediment sizes in the flume studies ranged from 0.19 to 0.93 mm, with maximum sizes up to approximately 1.7 mm (Guy et al., 1966).
- Meyer-Peter and Müller (MPM) (1948), a bedload function developed primarily from experimental data having well-graded sediments with median size up to 29 mm.
- MPM-Toffaleti, is a total load function for sand and gravel bed streams. Sediment transport is calculated using both functions by size class. Calculated bed load from the Toffaleti (1968) function is compared to the total calculated by MPM and the larger is used for bed load. Suspended load is then calculated using Toffaleti and added to the predicted bed load. This combined function is an approach to reduce the tendency of the Toffaleti function to grossly under predict transport of coarser sediments by replacing Toffaleti's empirically calculated bed zone transport with transport calculated using MPM.
- Yang (1973 and 1984), a total load function based on flume and field data that couples Yang's (1973) function for total load of sand-sized sediment with Yang's (1984) function for total load of

gravels. The 1984 function was developed from flume studies of nearly uniformly graded gravels with median size of 2.5 mm (Casey, 1935), 3.2 mm, 4.9 mm, and 7.0 mm (Gilbert, 1914).

A transport function should be selected that was developed for similar gradations and hydraulic conditions as found in the project of interest. Two important distinctions are evident in the available transport functions: (1) total load versus bed load, and (2) development using sand-dominated sediment versus sand gravel mixtures. Given the sampled and observed bed materials, it is reasonable to expect that the abundance of sand is transported as both bed load and suspended load. Thus, the suspended bed material load is significant in the project area and a total load function is preferred. Of the three remaining total load functions, the Yang (1973 and 1984) equation was developed using data that matches the bed material and hydraulic characteristics of the project reach, and has been used successfully by the project team for similar studies and was therefore selected for use in the sediment-transport analysis.

6.3 Sediment-transport Rating Curves

Reach-averaged hydraulic data and the censored (without silt/clay) bed material gradations were used as input to the Yang equation to develop total bed-material transport-capacity rating curves for the supply and downstream reaches. Two specific reaches were considered in the analysis, including:

- The 600-foot reach that represents the upstream sediment supply to the culvert extending from approximately Model Station (Sta) 2600 to 2000. This reach appears to be generally in equilibrium with the upstream sediment supply and thus represents the sediment supply to the bridge crossing.
- The 600-foot reach that represents the downstream channel below the culvert extending from approximately Model Station (Sta) 1700 to 1800. This reach is downstream from the plunge pool and over-steepened apron below the crossing and appears to be representative of the channel that would be subject to long-term channel degradation associated with a potential deficit in upstream sediment supply.

The reach-averaged hydraulic conditions were developed from the proposed-conditions model results for each reach by averaging the primary hydraulic variables (velocity, depth, top width, and hydraulic roughness for the main channel) and back-computing the reach-averaged slope from the resulting average hydraulic variables.

The bed-material sediment-transport capacity rating curves were developed using the SAMWin computer program that, among other things, computes the sediment-transport capacity based on an input sediment gradation and hydraulic conditions (main channel velocity, depth and top width, energy slope, and water temperature) over a range of discharges. For comparative purposes, sediment rating curves were also developed at the up- and downstream faces of the crossing and through the opening. The resulting sediment rating curves are shown in **Figure 6-2**. These curves indicate that the capacity of the downstream reach exceeds the sediment supply over the range of modeled flows. The curve at the upstream face of the culvert shows higher sediment loading due to the relatively steep inlet to the culvert, and the curve at the downstream face shows a reduction in sediment loading (at the higher discharges) associated with flow expansion and reduced energy gradients at the culvert outlet. Sediment transport capacity through the culvert is comparatively low but may be artificially so since the model results do not account for turbulent flow conditions in the culvert.

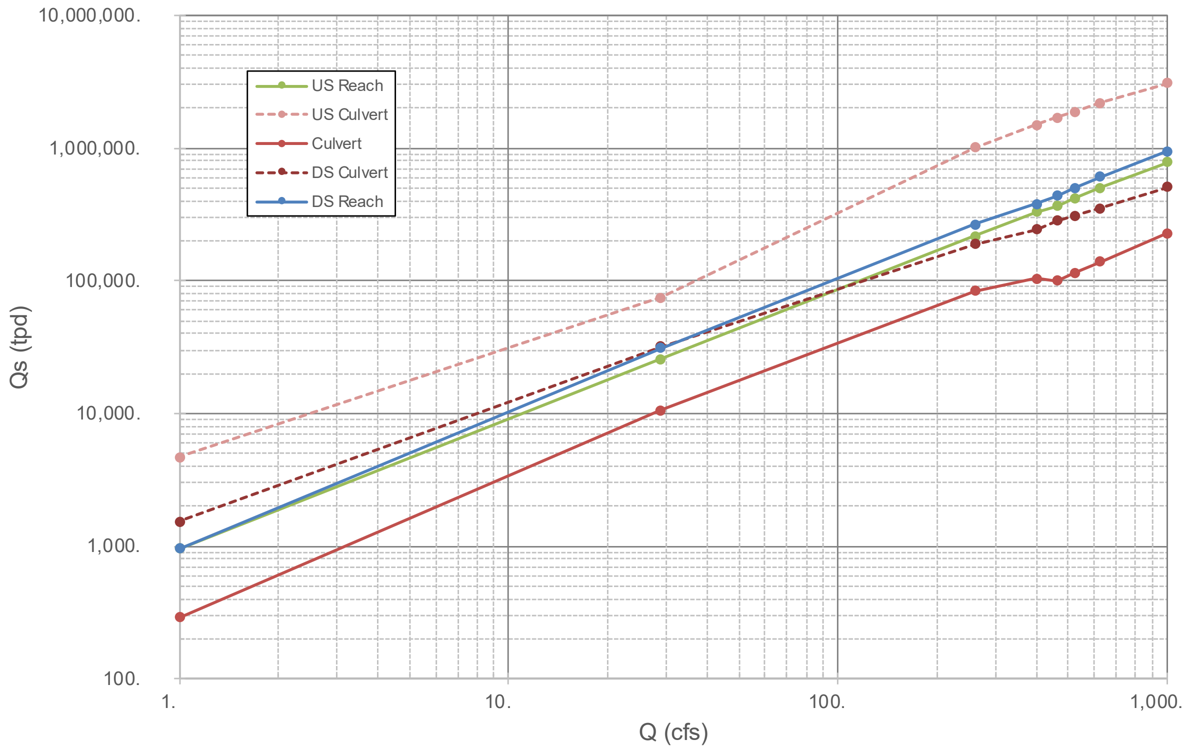

Figure 6-2 - Computed bed material sediment-transport capacity rating curves for the upstream supply reach and the reach downstream from the bridge crossing. Also shown are the rating curves at the up- and downstream culvert faces and through the culvert.

6.4 Sediment-continuity Analysis

The sediment-continuity analysis was performed by comparing the sediment-transport capacity of the reach downstream from the culvert to the sediment supply from the upstream reach. Where the transport capacity of the downstream reach exceeds the supply, the channel will respond by either degrading (i.e., channel downcutting), widening or coarsening its bed material (or some combination thereof), and where the supply exceeds the capacity, the channel will respond by aggrading, narrowing or fining its bed material (or some combination thereof). It should be noted that significant amounts of downcutting, aggradation or armoring can also lead to lateral instability that is not directly addressed by the continuity analysis. It should also be noted that the results from this continuity analysis represent the existing channel geometry in the project reach and do not factor in the complex responses of future aggradation, degradation and channel width adjustment. Therefore, the results do not reflect future changes in channel geometry and slope that would occur as a result of aggradation or degradation.

To perform the continuity analysis, the sediment rating curves discussed in the previous section were converted to volumes of sediment by integrating the curves under the 1-hour, 6-hour and 24-hour 100-year storm events discussed in **Section 3.0**. The results are presented in **Figure 6-3** and indicate that some degree of degradation is indicated downstream from the bridge crossing under each of the three modeled storm events. To put the predicted volumes of degradation in perspective, the volumes were converted to degradation depths over the approximately 1,800-foot reach between the bridge and the point where the channel becomes undefined at the dirt road crossing near model station 7+50. The most substantial amount of degradation would occur under the 24-hour, 100-year event, when the capacity below the bridge exceeds the supply by about 7,900 CY (degradation depth of 6.6 feet). Relatively moderate degradation is indicated under the 6-hour, 100-year event, when the capacity below the bridge exceeds the supply by about 4,900 CY, resulting in about 4.1 feet of degradation. The capacity exceeds the supply by about 3,100 CY (or about 2.6 feet of degradation) under the 1-hour, 100-year event.

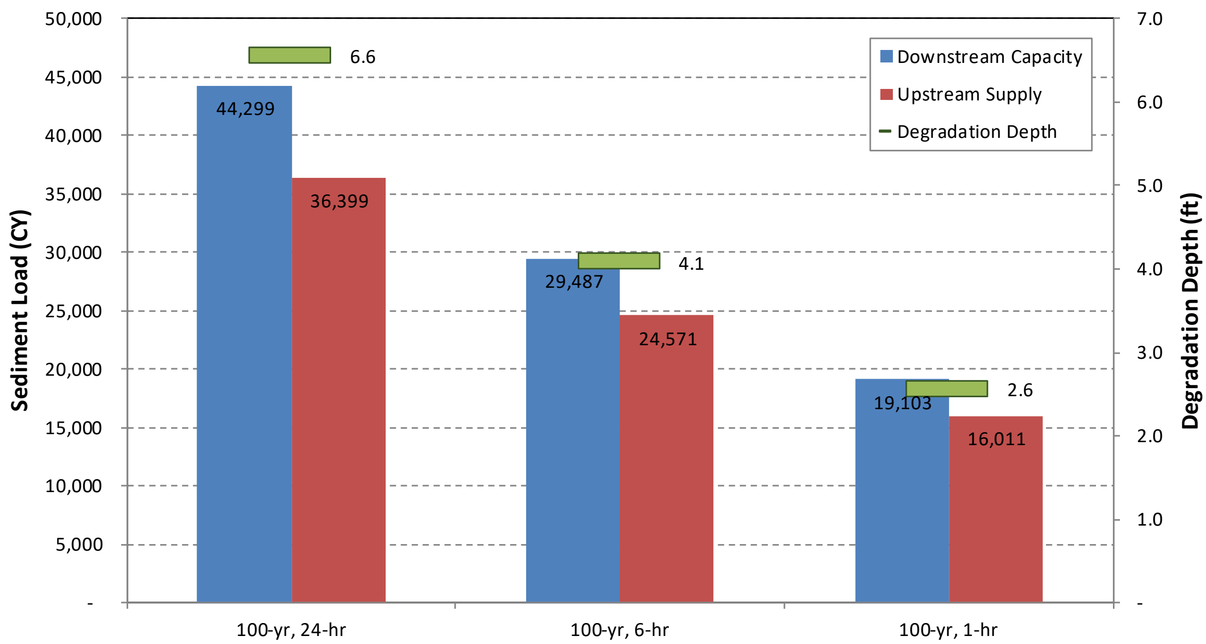

Figure 6-3 - Computed bed material sediment supply and transport capacity of the reach downstream from the bridge crossing, and the resulting estimated long-term degradation depth below the crossing.

The results from the sediment-continuity analysis indicate that up to 6.6 feet of long-term degradation could occur (24-hour,100-year event).

6.5 Sediment Laden n-values

To determine an appropriate n-value for the bridge undercrossing where concrete will be exposed during large events that scour out sediment (noted in Section 4.4), an analysis was conducted using a series of empirical equations. For the fully concrete-lined channel section transporting sediment, the Manning's n value can be estimated by (Copeland 2000):

$$n_{bedload} = 0.017 + 1.032 \times 10^{-6} C_{ppm}$$

Where,

$n_{bedload}$ = Manning's n value due to bedload

C_{ppm} = bed-material sediment concentration, in parts per million (ppm)

The bed-material discharge can be estimated by MPM equation (Meyer-Peter and Muller 1948):

$$Q_b = 0.0558[\gamma_w RS - 0.047(\gamma_s - \gamma_w)D_{50}]^{1.5} \times W$$

Where,

γ_w = Weight of water (62.4 lb/ft^3)

R = Hydraulic radius of flow (feet)

S = Energy slope, for backwater calculations; or bed slope, for normal depth (ft/ft)

γ_s = Weight of sediment (assumed 165.36 lb/ft^3)

D_{50} = Median diameter of sediment, by weight (feet)

W = Effective flow width (feet)

This form of the MPM equation will always yield conservative (i.e., safe) results, because it presumes that the grain roughness is dominant, and essentially represents the total roughness of the channel.

Once Q_b is determined, the bed-load portion of the bed-material sediment concentration, in ppm, can then be estimated by (Zeller 2014):

$$C_{ppm} = 1.0 \times 10^6 / \left(1 + 0.3774 \left[\frac{Q_w}{Q_b}\right]\right)$$

Where,

Q_w = Design discharge in cfs

Q_b = Bed-material discharge in cfs

The final results using the discharge, design, and sediment characteristics as input parameters determines the n-value of the concrete undercrossing while laden with sediment to be 0.023.

6.6 Historical Geomorphic Review

A field visit in March of 2020 showed accumulated sediment in the existing culvert (the culvert bottom was buried) that was experiencing some recent cutting (1-2 feet) that was not sufficient to expose the culvert bottom. Immediately upstream and downstream of the culvert there was 1-3 feet of local scour, but no long-term signs of degradation further upstream or downstream were observed. The site visit review suggests an alternating pattern of aggradation and sedimentation around the existing culvert.

A review of historical topo and aerials was conducted to look for any longer-term channel changes. A review of USGS aerials from 1972 and 1981 compared to present day show the same bridge crossing, though an older culvert as the current as-builts are dated 2002, but with a wider sandy channel downstream in the past. No significant lateral movement was identified with the channel. For topo, sources included the USGS quad map, a 1966 topo map, a 2004 topo map, and the current 2014 liDAR data. The USGS topo did not have sufficient resolution to make any judgements on vertical change. In the 1966 topo one can see a channel existing where there currently is one, with no alignment change. However, the resolution is not sufficient to identify local entrenchment patterns if any. The 2004 and 2014 LiDAR shows no lateral change either and the topo is inconclusive regarding vertical changes from apparent burning in of flowlines in post processing.

7.0 Debris Analysis

Consideration of debris loads carried by streams below mountain and foothill areas is essential in the planning and design of flood control works. Unfortunately, this is one of the least understood, and most often neglected areas of flood control engineering. Failure to provide either debris storage facilities, or additional hydraulic capacity for debris bulked flows, could seriously affect the performance of flood control structures downstream of mountain and foothill watersheds.

Criteria for debris basin design is usually based on providing storage capacity for debris generated by a single major flood event at the minimum. Additional (or in some cases less) capacity may be provided depending on the physical constraints of the site.

Both Riverside County debris estimation method (RCFC&WCD 1978) and USACE Los Angeles District Method for Prediction Debris Yield (USACE 2000) were used in the following debris yield analyses. The former provides guidance for an annual average estimation, then refers to using the latter for single event yield estimations.

7.1 Riverside County Annual Average Estimation

The following are extracted from the Riverside County Hydrology Manual (RCFC&WCD 1978):

> *A report titled "Factors Affecting Sediment Yield and Measures for the Reduction of Erosion and Sediment Yield" may be useful in estimating average annual debris production rates in the District, or in adjusting data from adjacent areas to conditions in Riverside County. This report dated October 1968, was developed for areas in the Pacific Southwest by the Water Management Subcommittee of the Pacific Southwest Inter-Agency Committee.*
>
> *Based on long term records (30-years or more) from Los Angeles County, average annual debris production rates range from 700-cubic yards to 12,000-cubic yards per square mile for one-square mile watersheds in the San Gabriel Mountains. The average annual rate in these watersheds is approximately 6,450-cubic yards per square mile (about 4 acre-feet) for a one square mile watershed.*
>
> *Average annual debris production rates in Riverside County are generally believed to be lower than those experienced in the western San Gabriel Mountains.* It may be possible to estimate average annual debris production rates for watersheds in Riverside County by using data developed in the Los Angeles area, and accounting for geologic and hydrologic differences.

Per Plate F-1 of Riverside Hydrology Manual (RCFC&WCD 1978), the upper enveloped annual average debris yield of Gilman Springs Road crossing is estimated to be 86,350 cubic yards (53.3 acre-feet) for its drainage area of 0.66 square miles (see Appendix E).

The RCFC&WCD debris method approach is an estimated debris potential over an entire rain season, useful for designing debris basins that may need to be excavated on an annual basis. Additionally, unburnt watersheds produce lower volumes of debris than watersheds that have been recently burnt, and this methodology does not have a fire factor parameter that can influence the expected debris yield in a given year related to the year of burn. The USACE method that follows functions for single storms, better suited to the design this report is evaluating that has no debris basin, as well as accounting for fire impacts.

7.2 USACE Los Angeles Debris Method

The USACE Los Angeles Debris Method (USACE 2000) is intended to be used for the estimation of debris yield mainly from coastal-draining, mountainous, Southern California watersheds. The primary objective the method is to estimate unit debris yield values for "n-year" flood events for the design of debris-catching structures in coastal Southern California watersheds, considering the coincident frequency of wildfire and flood magnitude. Outside of the area from which the data were taken (San Gabriel Mountains), application of the Adjustment/Transposition (A-T) Factor must be carefully applied. Conditions different from those of the San Gabriel Mountains needs to be addressed. Because vegetation types and density are far different in desert-draining than coastal-draining watersheds, the effects of wildfire will not be the same. Additionally, the Fire Factor (FF) variable, which accounts for the impact of wildfire on debris yield from these watersheds, must also be carefully applied.

Regression Equation 1 was selected by statistical criteria for use in watersheds from 0.1 to 3.0 mi^2 in area for which peak flow data is not available. Equation 1 takes the form:

$$LOG\ Dy = 0.65\ (LOG\ P) + 0.62\ (LOG\ RR) + 0.18\ (LOG\ A) + 0.12\ (FF) \quad \ldots\ \textbf{Eq. 1}$$

where:

Dy = Unit Debris Yield (yd^3/mi^2)

P = Maximum 1-Hour Precipitation (inches, taken to two places after the decimal point, times 100)

RR = Relief Ratio (ft/mi)

A = Drainage Area (ac)

FF = Non-Dimensional Fire Factor

The coefficient of multiple determination for this equation is 0.987. All factors in this equation are significant at the 0.99 level of confidence. A total of 349 observations from 80 watersheds were used in the final development of this equation.

Gilman Springs Roadway crossing debris estimates of n-year storm events are presented in **Table 7-1** and **Table 7-2** with watershed burned in the prior year (FF = 6.5) and watershed burned more than 10-years ago (FF = 3) with A-T factor of 1 as a conservative measure.

7.3 Debris Storage Potential

The upstream approach to the existing and proposed bridge could potentially act to absorb and contain some portion of debris that may be generated in a storm event. The topographic mapping provided for the hydraulic analysis was subsequently used to estimate the volume of area upstream of the top of the bridge deck to compare that area's volume against the calculated potential debris yield found in **Table 7-1** and **Table 7-2**.

Figure 7-1 shows the potential 'storage' area upstream of the bridge, which has been calculated within the footprint shown, to be equal to 723 cubic yards, or 0.46 acre-feet. Debris that exceeds this volume in a debris flow will overtop the bridge if it is incapable of passing beneath it.

The debris estimates provided in Section 7.0 are for information purposes only since no debris capture structure is proposed in this study or design, but may inform local operations and maintenance of a potential need to clear the channel and crossing in case of a debris flow event.

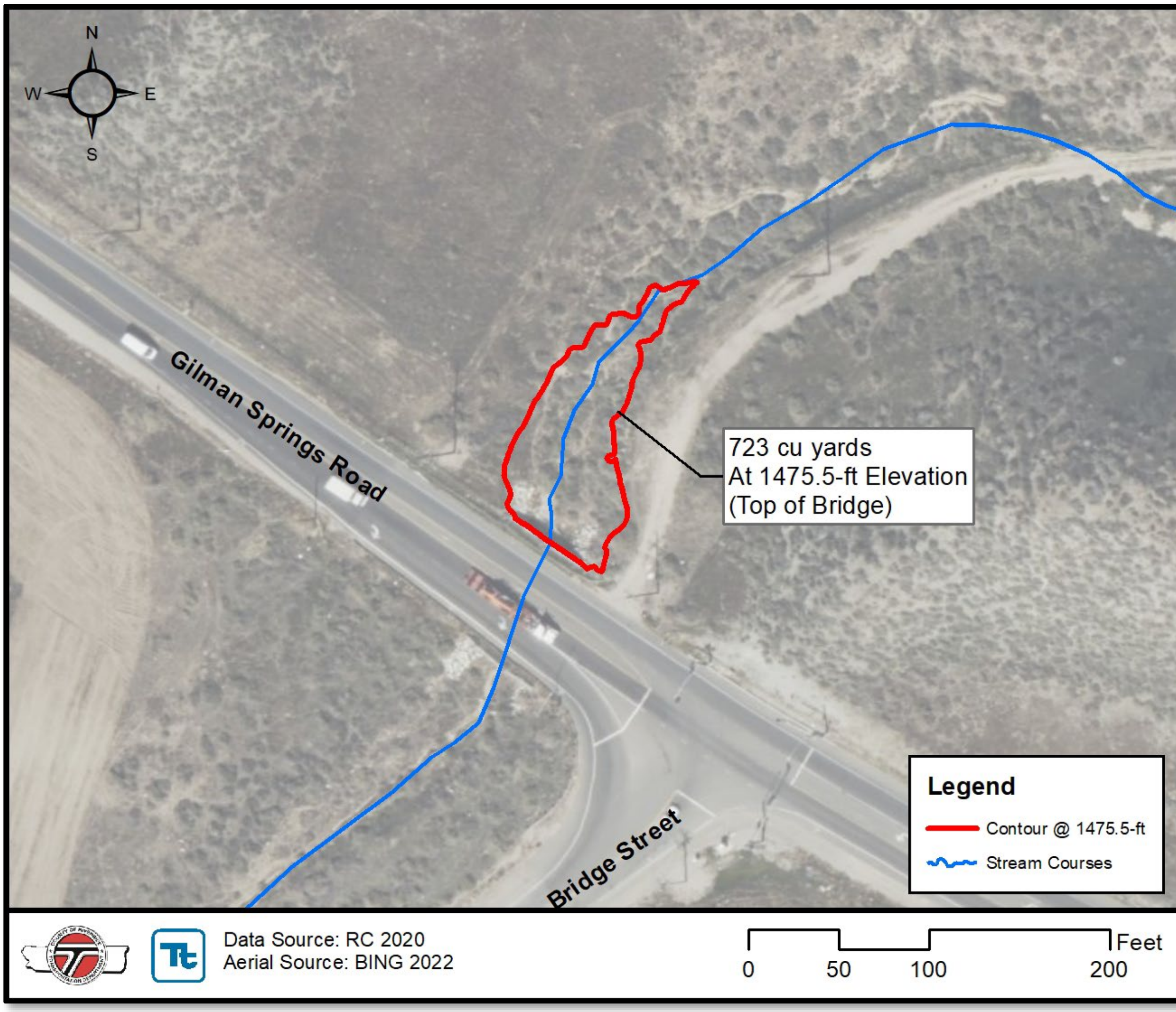

Figure 7-1 – Potential Debris Storage Area

Table 7-1 - Gilman Springs Roadway Crossing Debris Estimates (Watershed Burned in the prior year)

Area (Ac)	U/S Elevation (ft)	D/S Elevation (ft)	Water Course Length (ft)	Relief Ratio, RR, (ft/mi)	Adjustment and Transposition Factor, AT	Fire Factor, FF			
425.12	2200	1460	9088.12	429.92	1	6.5	<=Watershed burned prior year		
Frequency	**NOAA Atlas 14, 1-hr Precip (in)**	**Dy (yd^3/mi^2)**	**Log Dy =**	**0.65* Log P**	**+ 0.62 * Log RR**	**+ 0.18 * Log A**	**+ 0.12 * FF**	**Debris Yield (yd^3)**	**Debris Yield (ac-ft)**
1-yr	0.39	8318.16	3.92	1.03	1.63	0.47	0.78	***5,525***	***3.42***
2-yr	0.51	9902.75	4.00	1.11	1.63	0.47	0.78	***6,578***	***4.08***
5-yr	0.70	12166.04	4.09	1.20	1.63	0.47	0.78	***8,081***	***5.01***
10-yr	0.86	13907.83	4.14	1.26	1.63	0.47	0.78	***9,238***	***5.73***
25-yr	1.11	16417.06	4.22	1.33	1.63	0.47	0.78	***10,905***	***6.76***
50-yr	1.32	18374.20	4.26	1.38	1.63	0.47	0.78	***12,205***	***7.57***
100-yr	1.56	20481.72	4.31	1.43	1.63	0.47	0.78	***13,605***	***8.43***

Table 7-2 - Gilman Springs Roadway Crossing Debris Estimates (Watershed Burned in more than 10-years ago)

Area (Ac)	U/S Elevation (ft)	D/S Elevation (ft)	Water Course Length (ft)	Relief Ratio, RR, (ft/mi)	Adjustment and Transposition Factor, AT	Fire Factor, FF			
425.12	2200	1460	9088.12	429.92	1	3	<=Watershed burned 10+ yr ago		
Frequency	**NOAA Atlas 14, 1-hr Precip (in)**	**Dy (yd^3/mi^2)**	**Log Dy =**	**0.65* Log P**	**+ 0.62 * Log RR**	**+ 0.18 * Log A**	**+ 0.12 * FF**	**Debris Yield (yd^3)**	**Debris Yield (ac-ft)**
1-yr	0.39	3162.48	3.50	1.03	1.63	0.47	0.36	***2,101***	***1.30***
2-yr	0.51	3764.92	3.58	1.11	1.63	0.47	0.36	***2,501***	***1.55***
5-yr	0.70	4625.40	3.67	1.20	1.63	0.47	0.36	***3,072***	***1.90***
10-yr	0.86	5287.61	3.72	1.26	1.63	0.47	0.36	***3,512***	***2.18***
25-yr	1.11	6241.59	3.80	1.33	1.63	0.47	0.36	***4,146***	***2.57***
50-yr	1.32	6985.68	3.84	1.38	1.63	0.47	0.36	***4,640***	***2.88***
100-yr	1.56	7786.93	3.89	1.43	1.63	0.47	0.36	***5,173***	***3.21***

7.4 Peak Bulking Rates

The RCFC&WCD Hydrology Manual provides guidance for bulking flows that are laden with debris and sediment. The following analysis looks at whether the proposed design can pass the expected bulked flows estimated.

Debris volumes equal to the clear water volume have been recorded during major floods in Los Angeles County. This is equivalent to 100-percent bulking, or a bulking factor of 2. The RCFC&WCD hydrology manual references that Los Angeles County Flood Control District (LACFCD) has proposed relating the peak bulking rate to debris production volume by assigning the maximum observed bulking factor of 2 to the maximum observed single storm debris production rate of 120,000-cubic yards for a one-square mile area. Thus the peak rate bulking factor is expressed as (RCFC&WCD 1978):

$$F_b = 1 + [\frac{D}{120{,}000}]$$

where:

D = Design storm debris production rate for the study watershed in cubic yards per square mile

To account for uncertainty, LACFCD applies a factor of safety to be added to this relationship for design purposes. The computed peak bulking rates for n-year storm events with fire factors of 6.5 (watershed burned in prior year) and 3.0 (watershed burned more than 10-year ago) are presented in **Table 7-3**. With a safety factor of 0.25, the 100-year design bulking factor of 1.46 and 1.33 are recommended for the watershed with prior year burn condition and prior more than 10-year burn conditions, respectively.

Table 7-3 - Computed Peak Bulking Rates, Fb

Frequency	D[1] (yd^3/mi^2)	Fb	Fb x 1.25 FOS	D[2] (yd^3/mi^2)	Fb	Fb x 1.25 FOS
1-yr	8318.16	1.069	1.337	3162.48	1.026	1.283
2-yr	9902.75	1.083	1.353	3764.92	1.03137433	1.289
5-yr	12166.04	1.101	1.377	4625.4	1.039	1.298
10-yr	13907.83	1.116	1.395	5287.61	1.04406342	1.305
25-yr	16417.06	1.137	1.421	6241.59	1.052	1.315
50-yr	18374.2	1.153	1.441	6985.68	1.058214	1.323
100-yr	20481.72	1.171	1.463	7786.93	1.065	1.331
1. Watershed Burned in prior year						
2. Watershed Burned in more than 10-year ago						

Using the suggested bulking factor above of 1.46, applied to the 100-year 1-hr event discharge, the HEC-RAS model shows that velocities could increase by approximately 1.5 to 2 fps typically, while the WSEL would increase approximately 0.75-ft. The bridge has the capacity to pass a bulked flow without overtopping if there is no debris of exceedingly large size.

THIS PAGE INTENTIONALLY LEFT BLANK

8.0 Culvert Scour

In addition to the sediment transport analysis in **Section 6.0**, separate methodologies were utilized as well to paint the greatest picture of potential erosion and scour potential, whether at the stream level, or local scour level.

8.1 Downstream Outlet Scour

The U.S. Department of Transportation (USDOT) Federal Highway Administration (FHWA) Hydraulic Engineering Circular No. 14, 3rd Edition (FHWA-NHI-06-086, 2006), was referenced for the cohesionless soils culvert outlet scour equation 5.1 to estimate scour at the end of the downstream wingwalls:

$$\left[\frac{h_s}{R_c}, \frac{W_s}{R_c}, \frac{L_s}{R_c}, \frac{V_s}{R_c^3}\right] = C_s C_h \left(\frac{\alpha}{\sigma^{\frac{1}{3}}}\right)\left(\frac{Q}{g^{1/2} R_c^{2.5}}\right)^{\beta}\left(\frac{t}{316}\right)^{\theta}$$

where:

hs = depth of scour, ft

Ws = width of scour, ft

Ls = length of scour, ft

Vs = volume of scour, ft3

Rc = hydraulic radius at the end of the culvert (assuming full flow)

Q = discharge, ft3/s

g = acceleration of gravity, 32.2 ft/s2

t = time in minutes

σ = (D84/D16)0.5, material standard deviation

α, β, θ are coefficients (from FHWA Table 5.1)

C_h = drop height adjustment coefficient (from FHWA Table 5.2)

C_s = slope correction coefficient (from FHWA Table 5.3)

FHWA Table 5.1. Coefficients for Culvert Outlet Scour in Cohesionless Soils

	α	β	θ
Depth, h_S	2.27	0.39	0.06
Width, W_S	6.94	0.53	0.08
Length, L_S	17.10	0.47	0.10
Volume, V_S	127.08	1.24	0.18

FHWA Table 5.2. Coefficient C_h for Outlets above the Bed				
H_d[1]	Depth	Width	Length	Volume
0	1.00	1.00	1.00	1.00
1	1.22	1.51	0.73	1.28
2	1.26	1.54	0.73	1.47
4	1.34	1.66	0.73	1.55
H_d[1] is the height above bed in pipe diameters (no drop in proposed design)				

FHWA Table 5.3. Coefficient C_s for Culvert Slope				
Slope %	Depth	Width	Length	Volume
0	1.00	1.00	1.00	1.00
2	1.03	1.28	1.17	1.30
5	1.08	1.28	1.17	1.30
>7	1.12	1.28	1.17	1.30

The results of this equation for the downstream culvert scour are reviewed in the following section and are compared to the sediment analysis in **Section 6.0**.

8.2 Upstream Scour

With the bulked flow hydraulics, the maximum velocity upstream of the wingwall approach is 11.3 fps. Per the Los Angeles County Hydraulic Design Manual (LACFCD 1982, p.F-32), the velocity range of 10 to 15 fps would induce expected scour that would require an extrapolated cut-off depth of 8.6-feet.

8.3 Scour Results

The results of the sediment transport analysis 100-yr potential long-term degradation for the 1-hr, 6-hr, and 24-hr events are listed below in **Table 8-1** along with the calculated local culvert scour single event (100-yr 1-hr bulked) results.

Table 8-1 - Summary of Proposed Condition Scour

	1-hr 100-yr Long Term Δ (ft)	6-hr 100-yr Long Term Δ (ft)	24-hr 100-yr Long Term Δ (ft)	1-hr 100-yr Bulked Local Scour Δ (ft)	Combined Potential Scour (Long-Term followed by Short-Term)
Downstream Degradation/Scour	-2.6	-4.1	**-6.6**	**-13.1**	**-19.7**
Upstream Degradation/Scour	-2.6	-4.1	n/a	**-8.0**	**-8.0**

The system exhibits stability upstream of the proposed bridge, with signs of both aggradation and degradation, likely due to the current culvert acting as a grade control. Downstream of the existing culvert the field inspection showed minor scour from winter events at the time, but overall stability further downstream. Those conditions do not reflect the scour potential from infrequent high intensity events. Since the computed scour from the FHA equation below the bridge crossing is about 13 feet, and exceeds the potential long-term degradation depths, the scour protection measures should be designed for the local scour, while protecting against the potential long-term degradation.

THIS PAGE INTENTIONALLY LEFT BLANK

9.0 Rock Sizing and Recommendations

9.4 Rock Sizing

For rock sizing purposes, an evaluation was done at both the upstream and downstream ends of the project. **Table 5-2** shows average maximum flow velocity of 19.1 fps (feet per second) and averaged maximum flow depth of 3.0 feet and maximum flow velocity of 12.8 fps with average maximum flow depth of 3.4 feet of upstream and downstream of the proposed bridge, respectively.

USACE CHANLPRO (USACE 1998) program was used in estimating the riprap sizes. A summary of CHANLPRO results are presented in **Table 9-1** and the input/output files are provided in Appendix F. A revision to add bulked flow results was performed in HEC-RAS 6.1 rock sizing hydraulic design tool which replaces CHANLPRO.

Table 9-1 - Summary of Rock Sizes

Reach	Max Ave Flow Velocity, V (ft/sec)	Ave Max Flow Depth, Y (ft)	Base Width, W (ft)	Side slope, Z (H:V)	Minimum D_{50} (in)	Thickness (ft)
Upstream (at Wingwall)	19.1	3.0	23	2:1	No Stable Gradations	n/a
Downstream	12.8	3.4	23	2:1	32	4-ft
Downstream Bulked Flow	14.8	4.2	23	2:1	32	4-ft

There are no stable gradations found by the CHANLPRO program for the reach immediately upstream of the bridge. See Section 9.3.1 for recommendations.

Downstream of the bridge, a stable gradation is found if the design channel maintains its design condition for the 100-year 1-hr flow, as well as the 100-year 1-hr bulked flow. However, the bulked flow condition is near unstable and if in the long term the scour potential of ~6.6-feet occurs, the stone in place at the downstream end may be undermined, settle, and steepen. In such a scenarios velocities would be similar to or exceed those found at the upstream end (grouted stone) where the approach is steep (>19 cfs), and the rock in place will no longer offer sufficient protection, potentially allowing head cutting to reach the cutoff wall.

9.5 Recommendations

9.5.1 Assumptions

Note for the following design recommendations related to scour protection, some assumptions are built in. It is assumed that the downstream cumulative scour depth of -19.7-ft, found in **Table 8-1**, should not occur as the design cutoff wall, in conjunction with the proposed channel protection and required O&M maintenance, would not allow the channel to simultaneously experience long term degradation followed by the modeled 1-hr, 100-yr bulked, storm and resulting local scour. The following are related assumptions for the scour protection recommendations:

- Following environmental requirements, concrete is not allowed downstream of the bridge as a means of channel scour protection, though it would have been preferrable.

- Following environmental requirements, the extent and volume of rock channel protection is limited to the immediate area downstream of the crossing.
- The cutoff wall is designed to protect the crossing from long-term degradation if downstream scour protection is not maintained.
- The channel scour protection is designed to protect the channel from the short-term event scour.
    - Note that in the recommendations below, rock sizing and volume were increased based on preliminary hydraulic modeling, with a conservative assumption that long-term scour happens to occur that would steepen the grade of the rock protection if the degradation is not addressed in a timely manner by O&M, but also in the event of a bulked flow that increases scour rather than adds sediment/debris.
- O&M will properly maintain the channel if long-term scour begins to take hold.
- O&M will properly maintain the proposed grouted stone upstream of the new crossing.
- O&M will properly maintain the rock protection that is implemented to protect the channel from short term scour.

9.5.2 Upstream Recommendation

Based on the results of **Table 9-1**, a HEC-11 (FHWA 1989) review was conducted to recommend a grouted rip rap thickness (see **Figure 9-1**). It is recommended that the upstream channel revetment, upstream of the concrete wingwall, should be **grouted riprap with a thickness of 2.5 feet** per **Figure 9-1**. There is still potential for scour at the upstream end approach of the grouted stone, therefor **the grouted stone should have a toe-down cutoff of 8.6-ft** per the Los Angeles District Hydraulic Design Manual to prevent potential undermining at the upstream end. The system has a ready supply of sediment, so scour that forms during event peaks should fill at the tail of a storm or from future smaller storms. Additionally, the transition from the grouted stone to the concrete wingwall segment will be a weak point where velocities are highest. It is recommended that the proposed cutoff wall (6-ft depth. See design plans) at the upstream end of the concrete wingwall be kept/included should the grouted stone begin to break up over time.

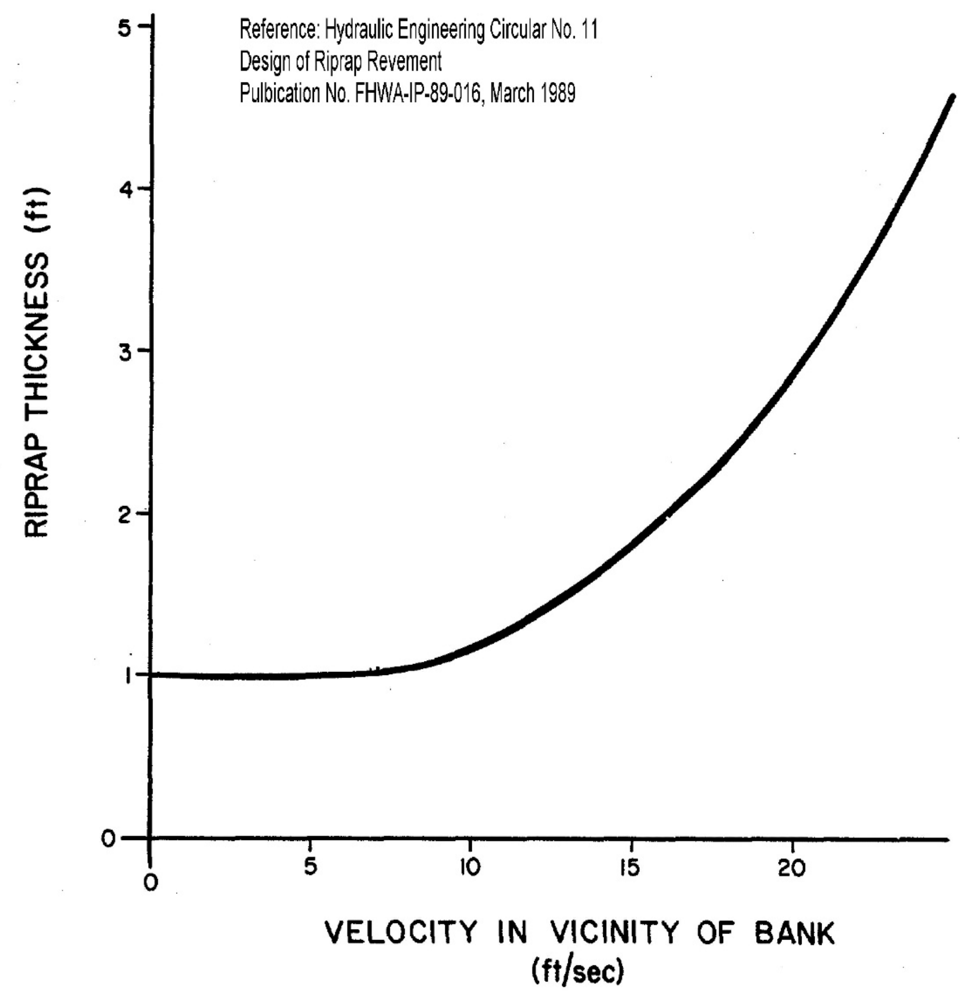

Figure 57. Required blanket thickness as a function of flow velocity.

Figure 9-1 - Grouted Riprap Thickness

9.5.3 Downstream Recommendation

At the downstream end of the system design, the calculated result is to utilize stone with a max D50 size of 32-inches, thickness of 4-feet, per **Table 9-1**, to protect against local scour from the 100-year 1-hr or 100-year 1-hr bulked storm at the bridge outlet. Note however that this stone does not protect against the downstream toe of the stone if it is undermined by the approximately 6.6-feet of longer-term scour event for the system downstream of the bridge (per **Table 8-1**). Should the longer-term scour event occur that promotes the stone to settle and drop, creating a steeper slope down from the wingwalls that promotes scour, velocities will be increased. In such scenarios, the velocities will be too high for the stone to be stable. Given environmental constraints over the protection design (no additional concrete), it is recommended to **increase the cutoff wall under the downstream concrete wingwalls to a depth of 9-feet**, **increase the size of the rock to D50**

36", and **increase the thickness of the rock layer to 4.5-feet, with the last 10-ft of downstream stone at 8-ft thick to function as launch stone should the toe of the stone begin to be undermined.** An example drawing is below in Figure 9-2 showing the downstream recommendations**.** The recommendations are both to provide additional protection and resistance against local scour (clear or bulked flow) if the rock is undermined or settles due to lack of maintenance and long term degradation, and also to provide additional response time for maintenance of the channel or rock, or addition to the rock, as needed. **Monitoring and maintenance as needed of the downstream channel and rock will be required to be added to regular O&M efforts by local responsible agencies.**

Figure 9-2 – Stone Protection Example

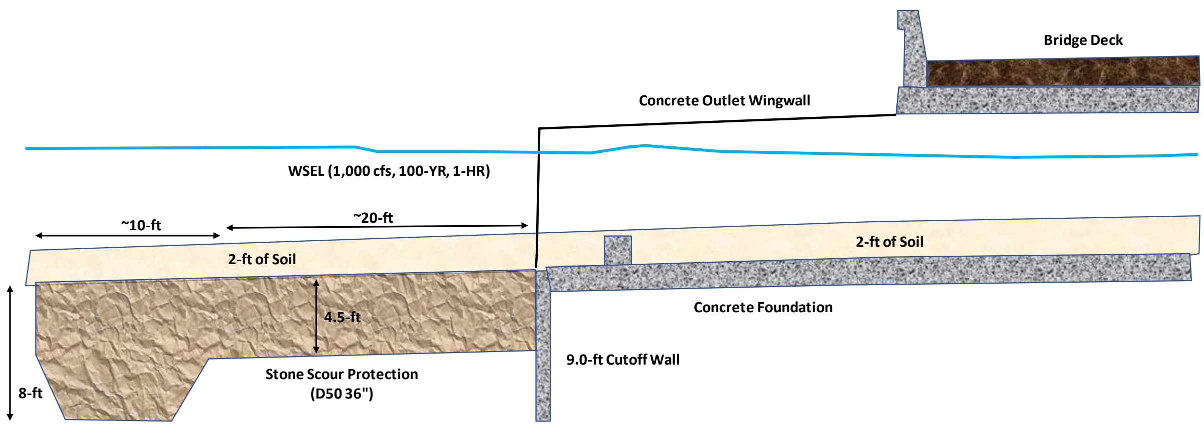

9.5.4 Soil Trap Recommendation

Lastly, given the goal to provide and maintain a soft bottom under the bridge for wildlife, which is reflected in the final grading plans, and given the scour potential of the flows entering under the bridge, a sediment trap is proposed to maintain the proposed design soil conditions under the bridge. This would consist of a 1.5 foot high, 1.5-foot wide concrete ledge/berm constructed across the channel, as part of the concrete foundation, 4.5-feet upstream of the end of the concrete channel/wingwall at the downstream end before the stone transition.

A sensitivity analysis was performed to evaluate the hydraulic impact of the sediment trap. The 2D model in Section 5.3 was modified to remove the sediment (~1.5-feet) underlying the bridge, which recognizes that the bed is mobile during large events, while adding the concrete ledge/berm. The result introduces a small hydraulic jump that does not increase the water surface due to the sediment being temporarily absent, while at the same time the jump reduces velocities downstream of the wingwall at the stone transition by 1-2 fps, while also allowing sediment at the tail end of smaller events to accumulate. The tail end of storms, as well as smaller events, will refill the soil under the bridge and it would extend all the way upstream to the base of the grouted stone on the north end of the bridge. This would facilitate continuous soil coverage of the concrete under the crossing. Additionally, the ledge/berm could be a bit higher, and a similar second one could be placed upstream as well if desired.

10.0 References

Arcement and Schneider 1989. Guide for selecting Manning's roughness coefficients for natural channels and flood plains. Water Supply Paper 2339. Colorado. United States Geological Survey (USGS).

Casey, H. J. 1935. Uber Geschiebebewegung. Mitt. Der Preuss. Versuchanst. Wasserbau und Schiffbau, No. 19. Berlin, Germany. (In German) as presented in Johnson, J.W. 1943. Laboratory Investigations on Bed-Load Transportation and Bed Roughness, A Compilation of Published and Unpublished Data. U.S. Department of Agriculture, Soil Conservation Service, Sedimentation Section, Office of Research, Technical Paper 50. Washington, D.C.

Copeland, R. 2000. Corte Madera Creek, Marin County, California, Modified Unit 4 Sedimentation Study, Numerical Model Investigation, August, 2000.

Cowan, W.L. 1956. Estimating hydraulic roughness coefficients: Agricultural Engineering, v.37, no.7.

Engelund, F.A., and E. Hansen. 1967. A Monograph on Sediment Transport in Alluvial Streams. Teknisk Forlag. Copenhagen. 62 p.

Gilbert, G.K. 1914. The Transportation of Debris by Running Water. U.S. Department of the Interior, Geological Survey, Professional Paper 86. U.S. Government Printing Office. Washington, D.C.

Guy, H.P., Simons, D.B., and E.V. Richardson. 1966. Summary of Alluvial Channel Data from Flume Experiments, 1956-61. U.S. Department of the Interior, Geological Survey, Professional paper 462-I. U.S. Government Printing Office. Washington, D.C.Hazen and Sawyer, P.C., Rondout Creek Hydrologic and Hydraulic Model for Water for the Future Program: Delaware Aqueduct Rondout-West Branch Tunnel Repair, Augmentation, and Modified Systems Operations DEIS., June, 2014.

Federal Highway Administration (FHWA). 1989. Hydraulic Engineering Circular No. 11 (HEC-11) Design of Riprap Revetment, publication No. FHWA-IP-89-016, March 1989.

Los Angeles County Flood Control District (LACFCD). 1982. Design Manual, Hydraulics. Los Angeles, CA. pp. F-32

Meyer-Peter, E. and R. Müller. 1984. Formulas for Bed-Load Transport. Proceedings of the second meeting of the International Association for Hydraulic Structures Research (IAHSR). Stockholm, Sweden. pp. 39-64.

National Highway Institute (NHI) 2006. Hydraulic Engineering Circular No. 14, 3rd Edition (FHWA-NHI-06-086). Maryland. Federal Highway Administration, US Department of Transportation.

National Oceanic and Atmospheric Administration (NOAA) 2014. NOAA Atlas 14, Precipitation-Frequency Atlas of the United States, Volume 6 Version 2.3: California. National Oceanic and Atmospheric Administration, National Weather Service, Silver Spring, Maryland, 2011, revised 2014.

Natural Resources Conservation Services (NRCS) 2011. National Land Cover Dataset, USDA-NRCS Geospatial Data Gateway <https://datagateway.nrcs.usda.gov/GDGOrder.aspx>, assessed on February 27, 2020.

Riverside County Flood Control and Water Conservation District (RCFC&WCD) 1978. Hydrology Manual, Riverside, California, 1978.

Riverside County Mapping Portal (RC) 2020. General Plan Landuse, GIS Database. <https://gisopendata-countyofriverside.opendata.arcgis.com/datasets/general-plan-landuse>

Thomas, W.A, Copeland, R.R., and McComas, D.N., 2002. SamWin Hydraulic Design Package for Channels. Prepared for U.S. Army Corps of Engineers, Coastal and Hydraulic Laboratory, Washington, D.C. by the USACE Engineer Research and Development Center, September.

Toffaleti, F.B. 1968. A Procedure for Computation of the Total River Sand Discharge and Detailed Distribution, Bed to Surface. U.S. Army Corps of Engineers, Committee on Channel Stabilization, Technical Report No. 5. Vicksburg, Mississippi.

United States Army Corps of Engineer (USACE)1998. User's Program for CHANLPRO, PC Program for Channel Protection Design, Engineer Waterways Experiment Station, July 1998.

United States of Army Corps (USACE) 2000. Los Angeles District Method of Prediction Debris Yield, Los Angeles District, California, revised February 2000.

Yang, C.T. 1973. Incipient Motion and Sediment Transport. ASCE Journal of Hydraulic Engineering, Vol. 99(HY10). pp. 1679-1704.

Yang, C.T. 1984. Unit Stream Power Equation for Gravel. ASCE Journal of Hydraulic Engineering, Vol. 110(12). pp. 1783-1797.

Zeller, M.E. 2014. Personal communication, (emailed to Chung-Cheng Yen, Tetra Tech, Irvine, California). [Michael Zeller, Principal Water Resources Engineer, Tetra Tech, Tucson, Arizona]

11.0 Appendices

A. Construction Drawing Sheets

B. Hydrology Output

C. Hydraulics Output

D. Scour Output

E. Debris Calculations

F. Riprap Calculations